American Mineralogist, Volume 78, pages 132–142, 1993

Melting experiments on a SiO_2-poor, CaO-rich aphanitic kimberlite from 5–10 GPa and their bearing on sources of kimberlite magmas

ALAN D. EDGAR, HEATHER E. CHARBONNEAU
Department of Geology, University of Western Ontario, London, Ontario N6A 5B7, Canada

ABSTRACT

Phase relations in a SiO_2-poor, CaO-rich aphanitic kimberlite from the Wesselton mine, Kimberley, South Africa, were determined in a multianvil apparatus at 5.0–10.0 GPa and 1300–1670 °C. The experiments were done with the 6.20 wt% H_2O and 4.77 wt% CO_2 ($X_{CO_2} \approx 0.24$) present in the rock. Olivine is the primary liquidus phase up to the maximum pressure investigated. An olivine + garnet + liquid assemblage is present at about 70 °C below the liquidus at low pressures to near-liquidus conditions at >100 GPa. No other primary phase is observed in these experiments, but a metastable (quench) phase resembling a high aluminum clinopyroxene occurs. Orthopyroxene is absent in all experiments, and the only carbonate phase is calcite, possibly a quench phase. In lower pressure experiments at 1.0–4.0 GPa, orthopyroxene was also absent, but primary clinopyroxene and calcite occurred, suggesting that their absence in this study may be the result of well-documented experimental difficulties with these phases in a multianvil apparatus.

The absence of orthopyroxene is not probably a result of decarbonation reactions such as those that occur in the peridotite-H_2O-CO_2 system, but it could possibly be the result of degassing during ascent of the Wesselton kimberlite, causing variation in the H_2O/CO_2 in this rock. The most likely reason for the absence of both orthopyroxene and a Mg-rich carbonate is that the bulk composition of this kimberlite has insufficient SiO_2 combined with high CaO relative to most kimberlites.

This study shows that the aphanitic kimberlite magma is unlikely to have equilibrated with a carbonated (magnesite or dolomite) garnet lherzolite or harzburgite in which orthopyroxene is an essential phase. Near-liquidus assemblages suggest that an olivine-bearing or olivine-free garnetite (garnet + clinopyroxene ± olivine), partially melted, is the most likely source to form this kimberlite. Furthermore, the depth of partial melting may have been considerably greater than the 150–250 km commonly accepted for kimberlite magma formation from a lherzolitic source.

Many kimberlites have the characteristic low SiO_2 and high CaO compositions found in the aphanitic kimberlite. If these kimberlites originate at the deep mantle levels suggested by this study, and if they have not been extensively changed by fractionation or loss of CO_2 on degassing, then they may be more likely to be diamondiferous, as they pass through a larger volume of potentially diamond-bearing mantle than kimberlites formed at shallower levels.

INTRODUCTION

Suprasolidus experiments were done at 5–10 GPa on a low SiO_2- and MgO-poor and CaO-rich aphanitic kimberlite from the Wesselton mine, South Africa. This study is an extension of earlier experiments up to 4.0 GPa performed on the same composition, in which the results indicated that a kimberlite magma of this composition may not have equilibrated with an assemblage containing orthopyroxene, i.e., a lherzolite or a harzburgite (Edgar et al., 1988). The objectives of the present study were to determine whether results of the lower pressure experiments could be extended to higher pressures and to assess the depth of origin and ascent path of such kimberlites.

Experimental data for kimberlites are scarce because of the difficulty in recognizing primitive kimberlite compositions: the rarity of kimberlites without xenocrysts and xenoliths, and, until recently, the absence of apparatus capable of attaining pressures equivalent to the depths of origin of kimberlite magmas. The nature and chemistry of the sources and the melting process to form kimberlite magma is very poorly constrained in models of kimberlite genesis (see Mitchell, 1986, p. 395).

ARE LHERZOLITES AND HARZBURGITES THE ONLY SOURCES OF KIMBERLITE MAGMA?

It is commonly accepted that all kimberlite magmas can be derived by partial melting of a carbonate-bearing (dolomite or magnesite) garnet lherzolite or harzburgite

0003–004X/93/0102–0132$02.00

on the basis of very extensive experimentation in model peridotite-H_2O-CO_2 systems (e.g., Eggler, 1975, 1978; Wyllie, 1977, 1978, 1979a, 1979b, 1980; Boettcher et al., 1980; Brey et al., 1984; Huang and Wyllie, 1984; Wyllie and Huang, 1976; Canil and Scarfe, 1990) that demonstrated the importance of CO_2 in forming dolomite and magnesite by carbonation reactions involving orthopyroxene. For example,

$$\text{olivine} + \text{clinopyroxene} + CO_2 = \text{orthopyroxene} + \text{dolomite} \quad (1)$$

$$\text{olivine} + \text{dolomite} + CO_2 = \text{orthopyroxene} + \text{magnesite} \quad (2)$$

$$\text{orthopyroxene} + \text{dolomite} + CO_2 = \text{clinopyroxene} + \text{magnesite}. \quad (3)$$

Loss of CO_2 from kimberlite melts favors olivine + clinopyroxene (Eq. 1). Hence, carbonated garnet lherzolite need not be the only source for kimberlite magmas, and, indeed, unequivocally carbonated (dolomite-magnesite) mantle samples are virtually unknown, the only possible exception being inclusions of calcite and possibly dolomite in garnet (McGetchin and Besancon, 1973).

H_2O is also essential for partial melting of likely sources of kimberlite magma. Phlogopite and amphibole are likely H_2O reservoirs, and both are relatively common in metasomatised mantle material (Lloyd, 1987). The compositions of partial melts of such mantle material is unknown because they cannot be quenched to a glass (Wendlandt and Eggler, 1980a) and, although they are probably K_2O-, MgO-, and carbonate-enriched, the extent depends on the degree of phlogopite and carbonate in the source.

Melting of model carbonated garnet lherzolite at high pressure (Wendlandt and Eggler, 1980b) and of a Lesotho kimberlite in which Co substituted for Fe in experiments carried out up to 5.0 GPa (Eggler and Wendlandt, 1979) suggested that kimberlitic melts may be formed at about 150 km. Canil and Scarfe (1990) experimented in the synthetic peridotite-CO_2 system up to 12.0 GPa and proposed that kimberlite magmas may form between 5.0 and 7.0 GPa and protokimberlite above 7.0 GPa. Experimental data imply that eutectic-like melting of phlogopite + magnesite + garnet + lherzolite (an assemblage containing essential orthopyroxene) at increasing pressures and degrees of partial melting can produce a series of melts whose compositions cannot be determined experimentally, but which probably range from carbonatite to carbonatitic kimberlite. Such melts, however, need not be in equilibrium with orthopyroxene in the source (see Canil and Scarfe, 1990, their Fig. 5a).

Are kimberlites primitive mantle melts?

Experiments on kimberlite compositions, as opposed to model (and actual) peridotite systems used to infer

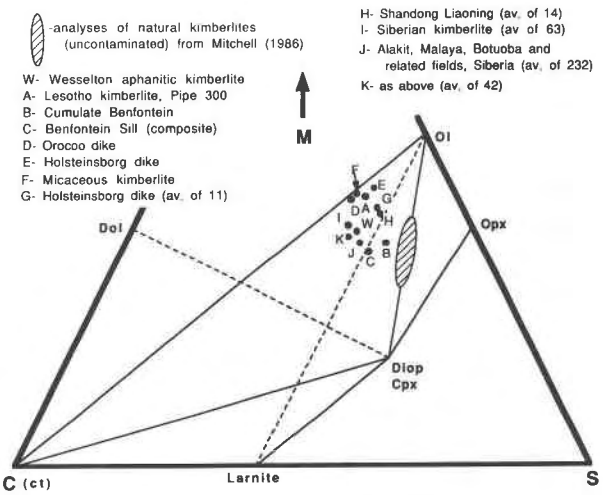

Fig. 1. Analyses of various kimberlites plotted on the CMS system. Uncontaminated kimberlites (Mitchell, 1986) plot along the tie line from olivine (ol) to diopside (Diop cpx) and may contain orthopyroxene (opx). Kimberlite compositions W and A–K are SiO_2-poor, CaO-rich kimberlites that are incompatible with opx and fall in the ol + cpx + ct (calcite) assemblage in this projection. W = Wesselton aphanitic kimberlite (this study), A–K = kimberlite from various localities given by Mitchell (1986, his Table 7.1). Full lines indicate stable assemblages, dashed lines represent incompatible assemblages.

lherzolitic or harzburgitic mantle sources for kimberlite magmas, are severely hampered by the inability to determine if kimberlite compositions represent actual melts, primitive or derivative. The abundance of xenoliths and xenocrysts in most kimberlites has probably modified compositions relative to the original kimberlite melt, and hence such kimberlites cannot be used for experimental studies.

Based on the absence of xenoliths and xenocrysts, and the kimberlite's fine-grained nature, Edgar et al. (1988) have argued that the hypabyssal facies aphanitic kimberlite (Clement et al., 1984) from the Wesselton mine, Kimberley, South Africa, may represent a composition close to that of a primitive kimberlite magma. Mitchell (1986) and Shee (1986) considered aphanitic kimberlites to be formed by near-surface flow differentiation or by crystal fractionation at depth. For the purposes of the present study, the actual origin of the Wesselton aphanitic kimberlite is not as important as the similarity in its composition to that of other kimberlites, some of which may be primitive.

The aphanitic Wesselton kimberlite is characterized by low SiO_2 and high CaO (Edgar et al., 1988, their Table 1), relative to many kimberlites (Mitchell, 1986). This composition and those of similar kimberlites (Mitchell, 1986, his Table 2) are plotted in the CMS system (Fig. 1) and fall within a narrow compositional range that is removed from the range of uncontaminated kimberlite compositions. None of the kimberlite compositions similar to the aphanitic variety is compatible with enstatite

(Fig. 1), and none contains normative hypersthene. Although the CMS system is very simplistic relative to the complex chemistry of kimberlites, the high CaO and very low SiO_2 in kimberlites, akin to that of the aphanitic kimberlite used in this study, make it highly unlikely that they were ever equilibrated with an assemblage containing orthopyroxene. The comparison in Figure 1 indicates that the aphanitic Wesselton kimberlite composition is reasonably representative of SiO_2-poor and CaO-rich kimberlites. The major difference between the aphanitic Wesselton kimberlite and the other kimberlites (Fig. 1) is its much lower $CO_2/(H_2O + CO_2)$. The effect of this on phase relations is discussed below.

Suitability of the Wesselton kimberlite for experimental studies based on its texture and the absence of xenocrystal olivine has been discussed by Edgar et al. (1988). The primitive value of 100 $Mg/(Mg + Fe_{tot}) = 83.9$, the values of Ni (810 ppm) and Cr (2410 ppm), and its similarities to the average of 44 other Group I kimberlites from Wesselton (Edgar et al., 1988, their Table 1) suggest the aphanitic kimberlite has not undergone appreciable fractionation, although some olivine or pyroxene fractionation is possible on the basis of the data in Figure 1 of this paper.

In previous experiments on the same kimberlite up to 4.0 GPa at $CO_2 \approx 0.24$ and 0.52, Edgar et al. (1988) did not find orthopyroxene in any experiment but found calcite as the only carbonate in the lower XCO_2 condition and dolomite only at temperatures well below that of the liquidus and at >3.5 GPa. On the basis of these experiments, Edgar et al. (1988) suggested that the Wesselton aphanitic kimberlite magma was not generated by partial melting of a source containing orthopyroxene, that the magma may have exceeded 1300 °C at depths equivalent to about 1.2 GPa, and that calcite was the only carbonate in the source.

Experimental and analytical techniques

All experiments were done on a USSA-2000 fully automated uniaxial, split-sphere multianvil apparatus at the University of Alberta, Edmonton. The sample was placed in a Pt capsule that was 2.2 × 5 mm, predried at 120 °C, and welded shut. The capsule was then placed in the furnace assemblage, which consisted of a stepped graphite heater surrounded by a ZrO_2 sleeve, which was contained within a semisintered $MgO\text{-}Cr_2O_3$ (5%) octahedron of 12-mm edge length. The octahedron was then placed in a cavity formed by truncating the corners of eight WC anvils; the truncation edge length was 11 mm.

Temperatures were controlled to within ±5 °C of the values quoted by a Eurotherm 818P controller interfaced with a 80286 microcomputer. A $Pt\text{-}Pt_{87}Rh_{13}$ thermocouple placed axially and in contact with the tip of the sample capsule recorded the temperature. No correction was made for the effects of pressure on the emf output of the thermocouple. Independent measurements of the axial temperature profile at the center of the furnace indicated that the center of the sample may be ~10 °C hotter than the ends of the capsule, where the temperature is measured.

Pressure was calibrated at room temperature at the phase transitions BiI-BiII at 2.55 GPa (Hall, 1971) and BiII-BiV at 7.7 GPa (Holman, 1975). At 1000 °C, the calibration was based on the transitions: quartz-coesite at 2.95 GPa (Bohlen and Boettcher, 1982), fayalite-spinel at 5.27 GPa (Yagi et al., 1987), garnet-perovskite at 6.1 GPa for the composition $CaGeO_3$ (Susaki et al., 1985), and coesite stishovite at 9.1 GPa (Yagi and Akimoto, 1976). The estimated pressure uncertainty is <0.5 GPa.

The experiments were quenched by shutting off the power while the pressure was maintained by simultaneous pumping by the automatic pressure control system, thus approximating an isobaric quench. With this procedure, the temperature dropped to below 200 °C in under 2 s. Pressure was then decreased at 1–1.5 GPa/h.

The experiments took place with only the volatiles present in the kimberlite (6.20 wt% H_2O; 4.77 wt% CO_2), equivalent to $X_{CO_2} = 0.24$ [where $X_{CO_2} = CO_2/(CO_2 + H_2O)$ mol], the same value as that used in some of the lower pressure experiments (Edgar et al., 1988). Both prior to and after the experiment, the capsule was weighed to assess any likely loss of volatiles. In two instances of weight loss, the capsule was discarded. The experiments are assumed to have been done under volatile-absent conditions, based on the reasons described by Edgar et al. (1988).

Short experiment durations and the presoaking of the Pt capsules with Fe (Ford, 1978) are believed to minimize Fe loss from the kimberlite caused by alloying with the Pt capsule. No quantitative assessment can be made of the amount of Fe lost by alloying, but Mg′ [100 $Mg/(Mg + Fe_{tot})$] of minerals crystallized under similar temperature conditions as those in the lower pressure experiments (Edgar et al., 1988) suggest that some Fe loss occurred, on the basis of the high Mg′ of olivine (3.5 GPa, 1350 °C, Mg′ 94 (Edgar et al., 1988); olivine 5.0 GPa, 1300 °C, Mg′ 95). The values are similar to those of olivines crystallized at the liquidus at 1550 °C and at the same pressure from a dry peridotite by Takahashi (1986). In these experiments there was no Fe loss, and the f_{O_2} was likely lower. This comparison suggests that some Fe loss occurred in the present study and that the f_{O_2} was higher than in Takahashi's (1986) study. Part of the discrepancy, however, is accounted for by the lower Mg′ of the peridotite (Mg′ 79) relative to that of the aphanitic kimberlite (Mg′ 84).

No direct control of f_{O_2} can be made in these experiments nor can estimates of f_{O_2} and f_{H_2} be determined. The presence of carbonates in both the present and the lower pressure experiments suggests an f_{O_2} above that of the EMOC-EMOD buffer (Eggler and Baker, 1982) in the absence of graphite, which was not detected.

Mantle f_{O_2} values at P-T conditions are comparable with those of the present study. Bulanova (1986) sug-

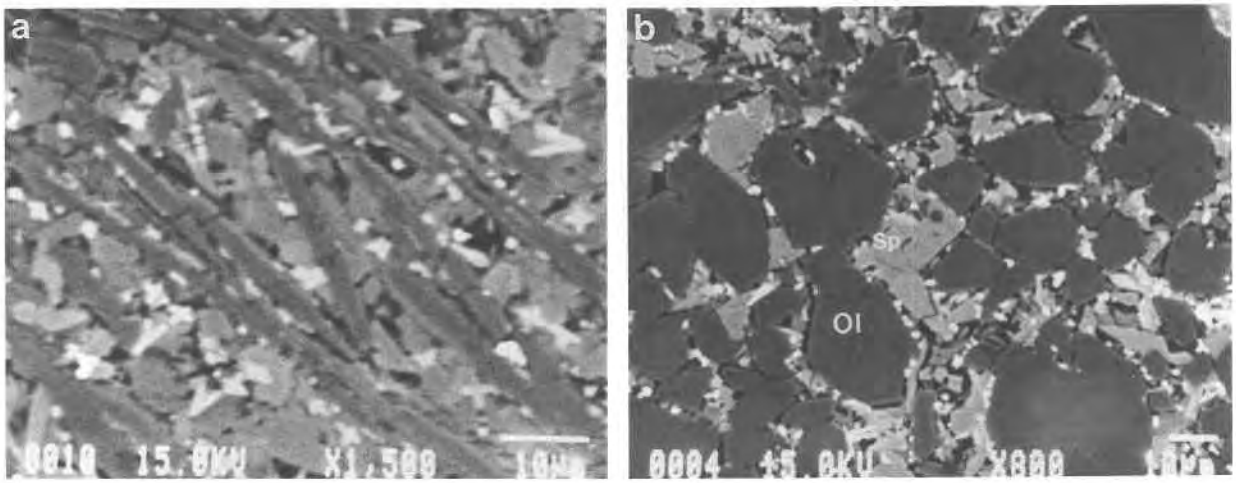

Fig. 2. Backscattered electron images of quench (**a**) and primary (**b**) products of experiments showing typical textures. Dark grains are olivine, gray grains are garnet, and lighter grains are the quench "clinopyroxene" (see text). Part **a** is from experiment no. 10 (Table 1) and Part **b** from experiment no. 17 (Table 1).

gested that f_{O_2} in diamond- and carbonate-bearing kimberlites ranged from that of the WM to the QFM buffer. More recently, Luth et al. (1990) have proposed a more oxidized mantle corresponding to an f_{O_2} between the QFM and WM buffers based on Fe^{3+} in mantle-derived garnets. The f_{O_2} values of both Bulanova (1986) and Luth et al. (1990) fall within the minimum possible f_{O_2} calculated by O'Neill and Wall (1987), on the basis of calculations involving the Ni content of olivine in equilibrium with orthopyroxene in a typical mantle peridotite. These studies suggest that the present experiments were done under higher f_{O_2} than those generally accepted for a peridotite mantle composition.

At the end of the experiment, the capsule was removed, embedded in epoxy, and sliced with a diamond saw. The surface was ground, and a polished thin section made for electron microprobe analysis. The products of each experiment were identified by EDS analysis and quantitatively by WDS analysis. Textures were observed by backscattered electron imagery.

In most experiments, the products consisted of quench material, composed of elongated crystals and blades of acicular olivine with interstitial garnet and a quench phase that resembled a very Al_2O_3-rich clinopyroxene (13–16 wt% Al_2O_3) (Fig. 2a), and of primary mineral assemblages with characteristic granuloblastic texture (Fig. 2b). The latter assemblage occurs close to the tip of the recording thermocouple, whereas the quench assemblage with spinifex-type texture (Fig. 2a) is observed farther away and indicates large thermal gradients along the capsule. No glass is detected in these experiments, as the melts have very low viscosities relative to those from the same compositions at lower pressures (<4.0 GPa). From these experiments, however, an estimate of the proportion of quenched melt to primary minerals may be made on the basis of the estimation of the proportions of granuloblastic aggregates near the thermocouple. In addition, the liquidus phase can be determined readily, as it is the first phase to appear at the boundary of the quench and primary parts of the charge (Fig. 3) Further distinction between primary and quench grains is based on the compositions of the minerals.

Minerals were analyzed on a Jeol 8600 electron microprobe on a four-spectrometer wavelength-dispersive system at an accelerating voltage of 15 kV and beam current of 10 nA. Several analyses (6–10) were made of each mineral considered to be primary.

Fig. 3. Backscattered electron image of boundary between liquid (quench) material at top of photograph and solid (primary) material at bottom of photograph, along which near-liquidus phases are present. Dark grains are olivine, lighter grains are garnet and quench "clinopyroxene." A few grains close to the boundary show garnet surrounded by olivine. Photograph from experiment no. 2 (Table 1).

TABLE 1. Results of experiments

Exp.	*P* (GPa)	*T* (°C)	*t* (min)	Products
10	10.0	1675	5	q-ol(93.0), q-g(79.6)
5	10.0	1600	15	ol(94.6), q-g(86.8)
2	10.0	1560	13	ol(94.4), g(90.4), q-"cpx", ap, sp(?)
15	10.0	1500	15	ol(91.0), g(78.4), q-"cpx", pv, Mg-ferrite, Mg-Ti-mt
12	9.0	1500	5	ol(94.1), g(81.6), q-"cpx", ap, ct
7	8.5	1600	15	ol(94.8), q-g(86.1) Mg-chr, ru
9	8.0	1500	15	ol(94.0), g(83.1), pv
14	8.0	1400	13	ol(93.1), g(81.0), q-"cpx", ap, ct
11	7.0	1540	5	ol(94.0), q-"cpx", cr-sp, Mg-ferrite, ap, pv
8	7.0	1360	16	ol(92.5), g(78.4), q-"cpx", Mg-Ti-mt, pv
6	6.0	1530	15	ol(94.9), q-g(78.8), q-"cpx", Mg-Ti-mt, Mg-chr, ap
3	6.0	1480	15	ol(94.2), g(83.3), q-"cpx", Mg-Ti-mt, ap, ct, pv
13	6.0	1425	20	ol(93.5), g(76.9), q-"cpx", ap, ct
17	5.0	1300	15	ol(92.5), g(76.4), q-"cpx", sp

Note: Abbreviations: q = quench, ol = olivine, g = garnet, "cpx" = quench clinopyroxene-like phase (see text), ct = calcite, ap = apatite, pv = perovskite, Mg-ferrite = magnesioferrite, mt = magnetite, sp = spinel, Mg-chr = magnesiochromite. Numbers in parentheses represent average Mg′ from several grains. Only olivine and garnet are considered to be primary phases.

RESULTS

Phase relations

Table 1 lists the results of experiments between 5.0 and 10.0 GPa and 1300 and 1675 °C. Figure 4 shows the stable phase assemblages. Only garnet and olivine are considered to be stable, on the basis of their textural relationships and their Mg′ values, which decrease with decreasing temperature and which are based on the average of 4–20 analyses (normally >10). Wherever possible, grains were analyzed at the liquid-solid interface (Fig. 3) considered to represent near-liquidus phases (cf. Herzberg et al., 1990). Throughout the *P-T* conditions of these experiments, quench clinopyroxene was abundant, particularly in the *P-T* range of field C (Fig. 4). This mineral had consistently high Al_2O_3 contents and did not always exhibit textures that could distinguish it as primary or quench. However, the values of Mg′, when compared with those of primary olivine and garnet, were too low to indicate that the clinopyroxene was in equilibrium with either phase. For these reasons, the clinopyroxene formed in these experiments is considered to be quench (Table 1). No glass or orthopyroxene was detected in any of the experiments. The all-liquid field (Fig. 4, field A) was determined on the basis of quench textures (Fig. 2a) and on the Mg′ of olivine and garnet (Table 1) being lower than the Mg′ of the primary varieties of these minerals. For example, the olivine and garnet in the experiment at 10.0 GPa, 1600 °C, have Mg′ values of 94.6 and 86.8, respectively, whereas the experiment at 10.0 GPa, 1560 °C, has olivine and garnet with Mg′ values of 94.4 and 90.4, respectively (Table 1). On the basis of this criterion, the olivine is considered to be primary, but the garnet is considered a quench phase at the higher temperature. Both olivine and garnet are primary at 1560 °C. This conclusion appears to contradict the textural relations (Fig. 3) in the products of this experiment that show garnet surrounded by olivine and therefore suggests that garnet formed earlier than olivine. These lines of evidence clearly indicate that both phases are very close to the liquidus at 10 GPa (Fig. 4). Minor amounts of various spinels (chromite, magnetite, magnesioferrite), calcite, rutile, apatite, and perovskite occur unsystematically in the experiments (Table 1). For this reason they are considered to represent metastable quench material.

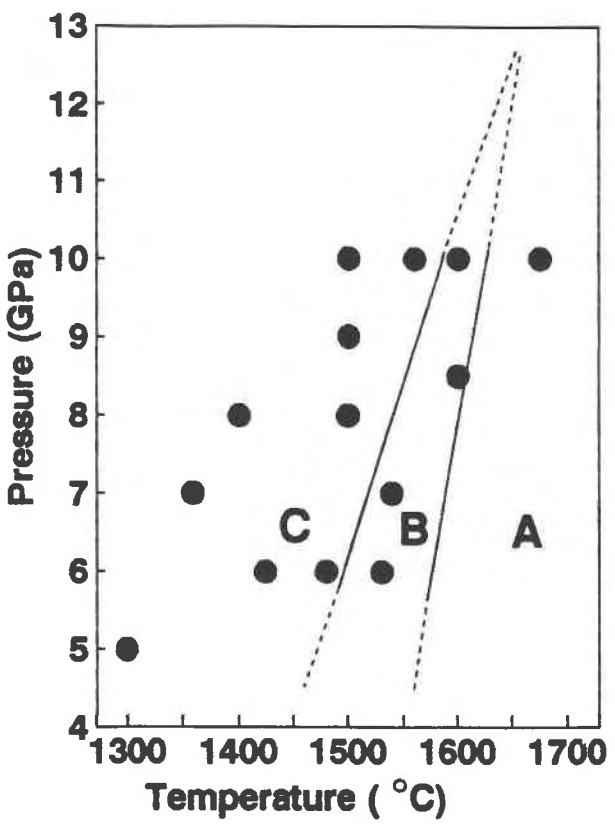

Fig. 4. Pressure-temperature relationships. Field A = all liquid, B = olivine + liquid, C = olivine + garnet + liquid. The quench "clinopyroxene" occurs in all fields but is most prominent in field C. Full lines represent well-established boundaries, dashed lines are extrapolated boundaries.

The boundaries in Figure 4 have been drawn based on

Table 2. Representative olivine analyses

P (GPa)	10.0	6.0	10.0	9.0	8.0	6.0
T (°C)	1600	1530	1500	1500	1500	1425
Major coexisting phases	—	—	g*	g*	g*	g*
Experiment no.	5	6	15	12	9	13
SiO_2	41.21	40.65	41.31	40.65	40.62	40.73
TiO_2	0.00	0.00	0.02	0.00	0.04	0.30
Al_2O_3	0.01	0.16	0.03	0.12	0.07	0.26
Cr_2O_3	0.00	0.30	0.00	0.05	0.00	0.39
FeO	5.51	5.62	6.54	6.24	7.49	6.21
MnO	0.04	0.12	0.16	0.08	0.00	0.28
MgO	52.32	53.21	52.45	52.94	51.96	52.07
CaO	0.24	0.30	0.28	0.21	0.25	0.44
Na_2O	0.00	0.00	0.14	0.00	0.00	0.00
NiO	nd	0.03	0.02	0.03	0.11	0.05
TOTAL	99.36	100.19	100.98	100.29	100.56	100.67
			Cations for 4 O atoms			
Si	0.997	0.979	0.990	0.980	0.982	0.979
$^{[4]}$Al	0.000	0.000	0.001	0.003	0.002	0.007
$^{[6]}$Al	0.000	0.000	0.000	0.000	0.000	0.000
Ti	0.000	0.002	0.000	0.000	0.001	0.008
Cr	0.000	0.001	0.000	0.001	0.000	0.007
Fe	0.111	0.113	0.131	0.126	0.151	0.125
Mg	1.887	1.909	1.873	1.902	1.872	1.856
Mn	0.001	0.002	0.001	0.002	0.002	0.004
Ni	0.000	0.001	0.001	0.001	0.000	0.001
Ca	0.009	0.008	0.007	0.005	0.006	0.011
Na	0.000	0.000	0.007	0.000	0.000	0.000
Mg′	94.4	94.3	94.3	93.7	92.4	93.5

Note: For abbreviations see Table 1.
* Coexisting garnet analyses given in Table 3.

the first appearance of primary minerals using Mg′. Hence the boundary between assemblages B and C is well constrained by experiments 5 and 3 (Table 1, Fig. 4). On extrapolation to higher pressures, this boundary meets the A-B boundary at about 12.0 GPa and thus represents the minimum pressure at which olivine and garnet coexist with liquid. On the basis of textural interpretation of garnet and olivine at the liquidus boundary (Fig. 3), garnet may be at the liquidus at as low as 10 GPa.

Mineral compositions

Tables 2 and 3 list compositions of olivine and garnet, where some of these minerals coexist (Fig. 4). The average Mg′ values for primary and quench phases used to construct the phase diagram (Fig. 4) are in Table 1.

In backscattered imagery (Fig. 2) olivine appears as dark angular grains that can be distinguished from frequently rounded garnet grains by a lighter color (Fig. 2b). Quench clinopyroxene has a color in backscatter imagery that is intermediate between that of olivine and garnet (Fig. 2b).

Representative olivine analyses are in Table 2. The Mg′ values of primary olivine are comparable with those in the lower pressure experiments (Edgar et al., 1988), with those of ultramafic assemblages, and with olivine phenocrysts in the Wesselton aphanitic kimberlites (Shee, 1986). The Mg′ values of olivine at the liquidus (Fig. 4) are slightly lower than predicted values for their high temperatures, suggesting that some Fe may have been lost.

Representative compositions of garnet are given in Table 3. The Mg′ of primary garnet is consistently lower than that of olivine (Table 1). The garnets are subaluminous, Ti-, Ca-, and Cr-rich members of the grossularite-pyrope-almandine series (Table 3).

The compositions of the garnets produced in the present experiments differ from those found in kimberlites and related rocks. Garnet is absent from the Wesselton aphanitic kimberlite (Shee, 1986) and in the lower pressure experiments (Edgar et al., 1988). The garnet compositions (Table 3) most closely resemble the Group 6 garnet, pyrope grossular almandine garnet, in the statistical classification of Dawson and Stephens (1975). These garnets are common in eclogites. The TiO_2 in the experimentally produced garnets is commonly greater (Table 3) than that of the megacrysts of Cr-poor garnets listed by Mitchell (1986). Megacryst garnets have lower CaO and higher FeO than those formed in this study.

Discussion

Nature of the source region for the Wesselton aphanitic kimberlite and compositionally similar kimberlites

The absence of orthopyroxene and primary clinopyroxene as suprasolidus phases in the experiments implies that, under the conditions used, liquid is not in equilibrium with a garnet lherzolite assemblage (garnet + olivine + orthopyroxene + clinopyroxene), and therefore this rock could not be the source of the kimberlite. Before considering the consequence of the absence of this assemblage, it is necessary to consider whether the absence of orthopyroxene is related to either the relatively low CO_2

Table 3. Representative garnet analyses

P (Gpa)	10.0	9.0	8.0	8.0	7.0	6.0
T (°C)	1500	1500	1500	1400	1360	1425
Major coexisting phase	ol	ol	ol	ol	ol, cpx	ol
Experiment no.	15	2	9	14	8	13
SiO_2	40.41	39.86	40.34	38.35	40.03	39.41
Al_2O_3	17.74	17.30	18.25	17.87	16.99	17.60
FeO	5.97	5.21	4.84	4.77	5.78	6.00
MnO	0.22	0.27	0.25	0.17	0.24	0.25
CaO	19.13	19.11	18.77	20.05	19.76	20.06
MgO	13.31	13.06	13.37	12.32	12.55	11.65
TiO_2	2.09	2.58	2.10	2.53	2.19	2.09
Cr_2O_3	1.98	2.32	2.22	2.42	2.30	2.00
TOTAL	100.85	99.21	100.13	98.51	99.84	99.06
Cations for 24 O atoms						
Si	5.943	5.925	5.939	5.789	5.966	5.978
$^{[4]}$Al	0.057	0.075	0.061	0.211	0.034	0.072
$^{[6]}$Al	3.017	2.955	3.103	2.968	2.950	3.048
Ti	0.231	0.288	0.232	0.287	0.245	0.236
Fe	0.734	0.648	0.598	0.602	0.720	0.755
Mn	0.027	0.034	0.031	0.022	0.030	0.032
Cr	0.230	0.273	0.258	0.289	0.271	0.238
Ca	3.014	3.043	2.961	3.248	3.155	3.233
Mg	2.918	2.893	2.934	2.772	2.788	2.612
Mg′	79.3	80.9	82.4	81.6	78.8	76.9
End-members						
Almandine	11.0	9.79	9.14	9.1	10.76	11.38
Spessartite	0.4	0.51	40.48	0.3	0.45	0.48
Grossularite	45.0	46.0	45.40	48.9	47.14	48.75
Pyrope	43.6	43.7	44.99	41.7	41.65	39.39

Note: For abbreviations see Table 1.

in the bulk composition or the possible elimination of orthopyroxene by reaction from a peridotite assemblage at pressures in the range of 5.0–8.0 GPa.

The absence of orthopyroxene

In their study of the aphanitic kimberlite up to 4.0 GPa, Edgar et al. (1988) attributed the absence of orthopyroxene in experiments at X_{CO_2} conditions of 0.24 and 0.51 to be caused by the lower SiO_2 composition of the aphanitic kimberlite relative to many other kimberlites (cf. Mitchell, 1986, his Table 7.3 and Fig. 1). They showed that the aphanitic Wesselton kimberlite plotted on the CMS and CMS CO_2 projections (Edgar et al., 1988, their Figs. 2, 3) was unlikely to have a composition compatible with an olivine + clinopyroxene + orthopyroxene source assemblage but pointed out that an SiO_2-poor melt might be derived from a partial melt of an olivine + clinopyroxene + orthopyroxene (lherzolite) source from which olivine ± orthopyroxene ± clinopyroxene had fractionated. There is little evidence, however, that the aphanitic kimberlite is a particularly evolved rock, rather than a primitive magma (cf. Edgar et al., 1988).

Alternatively a reaction relationship such as

$$\text{forsterite} + CO_2 = \text{enstatite} + \text{magnesite} \qquad (4)$$

may occur under higher X_{CO_2} conditions than those used in the present experiments. Studies of parts of the peridotite-CO_2-H_2O system (eg., Eggler and Wendlandt, 1979; Wyllie and Huang, 1976; Olafsson and Eggler, 1983; Brey et al., 1984; Canil and Scarfe, 1990) show that a reaction such as Reaction 4 will occur in the range of 3.0–4.0 GPa. No evidence of such a reaction occurs in either the relatively high X_{CO_2} experiments ($X_{CO_2} \approx 0.52$) of Edgar et al. (1988) up to 4.0 GPa or in the lower X_{CO_2} experiments above 5.0 GPa in this study, where no bona fide primary carbonate minerals occurred. The high amount of CO_2 required for Reaction 4 and other reactions is due to the necessity to saturate liquids in CO_2, based on experiments on the peridotite H_2O-CO_2 system, and hence is probably geologically unreasonable (cf. Mitchell, 1986). For example, more than 5% CO_2 is required to complete Reaction 1, and liquids in equilibrium with phases in the CMS-CO_2 system may have 35–40% CO_2, values in excess of any believed to be present in the mantle.

The possibility of orthopyroxene being a reaction product during peridotite melting at 5.0–8.0 GPa, and whether this melting can control the mineral relations of primitive melts, such as those of the aphanitic kimberlite, must be considered. Two reactions may take place in the presence of H_2O-CO_2 fluid:

$$\text{orthopyroxene} + \text{magnesite} + \text{clinopyroxene} + \text{olivine} + \text{fluid} = \text{melt} \qquad (5)$$

$$\text{olivine} + \text{magnesite} + \text{clinopyroxene} + \text{fluid} = \text{orthopyroxene} + \text{melt}. \qquad (6)$$

Reaction 5 involves a eutectic-like melting of a magnesite-bearing lherzolite source that could crystallize ortho-

pyroxene if the melt separated. Such a melt would also be expected to crystallize magnesite or dolomite at lower pressures. The absence of this type of carbonate composition in the low-pressure experiments of Edgar et al. (1988) and the total absence of any Mg-bearing carbonate phases, even in the quench experiments of this study, imply that the magma from which the aphanitic kimberlite formed was not derived from such a melt as modeled by Reaction 5.

If Reaction 6 is involved, then orthopyroxene might crystallize only briefly from the melt, after separation from the source, and any evidence of its presence would be difficult to detect. As in the case of the eutectic-like melt, however, the melt in this reaction might be expected to crystallize magnesite or dolomite at lower pressures. The absence of either of these minerals close to the liquidus in the low-pressure experiments (Edgar et al., 1988) suggests that the melt from which the aphanitic kimberlite evolved may not be due to Reaction 6.

Canil and Scarfe (1990) extended experiments on the model peridotite-CO_2 systems up to 12.0 GPa. They showed that partial melts from such a model peridotite at 5–7 GPa would crystallize orthopyroxene, whereas at >7 GPa a Mg-rich kimberlite magma (protokimberlite) might fractionate olivine at lower pressures, producing a primary kimberlite magma also in equilibrium with orthopyroxene (Canil and Scarfe, 1990, their Fig. 7). These authors believe that CaO-rich, SiO_2-poor kimberlites, such as the Wesselton aphanitic kimberlite, are the result of mixing of Si-poor and carbonate-rich melts at low pressure.

The absence of clinopyroxene

The absence of primary clinopyroxene in the products of the experiments is partly caused by experimental problems with such Mg-rich melts as the aphanitic kimberlite used in this study. Herzberg et al. (1990) have discussed this problem in detail and presented methods of obtaining analyses of equilibrium (primary) phases between near-solidus and liquidus conditions. The tendency of mixtures of quench and primary minerals to form as mattes containing both primary and quench material, particularly near the liquidus, was observed in nearly all the products of this study (Fig. 3). In many instances, clinopyroxene appears to be a primary mineral texturally but is in fact a quench phase grown around stable olivine and garnet. In no instance did microprobe analyses of clinopyroxene grains indicate that they were primary, as the Mg′ values were too low for the clinopyroxene to be in equilibrium with primary olivine and garnet (Table 1), and the Al_2O_3 contents (12–16 wt%) were much too high. Using these criteria, we do not consider clinopyroxene a stable mineral in these experiments.

Nevertheless the possibility of some clinopyroxene being primary, even close to the liquidus, cannot be excluded, and this idea receives some support from the presence of primary clinopyroxene in experiments up to 4 GPa (Edgar et al., 1988), in which problems in forming stable assemblages are not so great. Estimation of the compositions of residual liquids formed after the onset of garnet formation (Fig. 4, field C) certainly does not preclude clinopyroxene and some Al-bearing mineral (spinel?) as stable phases.

Similar arguments may apply to the absence of carbonate minerals, which texturally appear to be both primary and quench. Unfortunately no chemical criteria can be used to assess this. However, the only observed carbonate mineral is calcite.

The lack of unequivocal stable phases in the experiments does not alter the fact that orthopyroxene is not a likely mineral to be in equilibrium with a melt of the aphanitic Wesselton kimberlite composition under the conditions of this study.

Source for the aphanitic kimberlite magma

The source of the aphanitic kimberlite magma can be inferred from multiphase saturation of mineral phases at the liquidus or from near-liquidus phases. Figure 4 indicates that no multiphase saturation occurs, but garnet, along with olivine, is present near the liquidus at 10.0 GPa. If the lines representing the liquidus (first crystallization of olivine) and that of garnet (Fig. 4) are extrapolated to higher pressures, the assemblage garnet + olivine occurs at about 12–13 GPa. This assemblage is equivalent to a garnet dunite, an unlikely source for kimberlite because it is refractory. The presence of quench material of a composition equivalent to an Al-rich clinopyroxene up to the near-liquidus may modify this source material to that of a garnetite assemblage, a more likely candidate as a source of the aphanitic kimberlite magma. This multisaturation point on the extrapolated liquidus (Fig. 4) may imply that kimberlite magma arose by partial melting at pressures of 12.0–13.0 GPa.

The high pressure at which olivine is on the liquidus (Fig. 4) may be a consequence of the low X_{CO_2} in the experiments. Such a low value could be the result of loss of CO_2 during degassing of the aphanitic kimberlite. Thus, the relatively high H_2O or slight changes in the experiments increase the size of the olivine + liquid field (Fig. 4, field B), as demonstrated by Kushiro (1969) in the forsterite-diopside-SiO_2 system. If this is the reason for the stability of olivine to high pressures, then under a larger X_{CO_2} the multisaturation point involving olivine + garnet + clinopyroxene(?) might occur at lower pressures. The possibility that the aphanitic kimberlite is a result of localized large-scale melting of a garnet + clinopyroxene(?) assemblage, representing a garnetite of basaltic composition from a subduction-related process (Ringwood, 1989) such as that proposed for the Roberts Victor eclogites by Hatton and Gurney (1987), might exist. Some support for this suggestion may come from the similarity between the compositions of the garnets found in this study (Table 3) and those present in eclogites (see above). The garnets found in this study do not have the charac-

teristic high SiO_2 of very high pressure. Experiments on the eclogite-garnetite transformation (Irifune et al., 1989) indicate that SiO_2-poor garnets occur only above 10.0 GPa.

The experiments described here as well as those of Edgar et al. (1988) strongly suggest that the aphanitic Wesselton kimberlite did not evolve by partial melting of a garnet lherzolite but may have been derived by partial melting of a source that did not include orthopyroxene, or from which orthopyroxene was consumed during eutectic-like melting. The present study also suggests that formation of the magma from which this kimberlite formed could have occurred at a depth considerably greater than the range of 150–250 km for kimberlite magmas derived from carbonated garnet-lherzolite sources. If the olivine field in the experiments is decreased by a higher X_{CO_2} (see above), then the source inferred from the experiments may be at a depth equivalent to a pressure of <10.0 GPa (<300 km) or to a maximum pressure of 12.0–13.0 GPa (Fig. 4), equivalent to a depth of 350–400 km. If the source and depth of generation of the aphanitic kimberlite is due to its composition, as discussed above, then it is possible that kimberlites of comparable composition (see Fig. 1) may also have been evolved at deeper levels, and from similar sources, as the sample studied here.

The principal differences between the aphanitic kimberlite and those of comparable composition (Fig. 1 and Mitchell, 1986, his Table 7.3) is in the X_{CO_2}, which is higher for some of the kimberlites in Figure 1. Higher X_{CO_2} favors a shallower depth of melting (see above). The compositions shown in Figure 1 all fall within a narrow range when plotted on the CMS system and are not compatible with enstatite. The higher X_{CO_2} in these kimberlites (Fig. 1) may not change the source of SiO_2-poor CaO-rich kimberlite magmas, such as the Wesselton aphanitic kimberlite, but may be important in the depth of magma generation.

Canil and Scarfe (1990) suggested that kimberlites of similar compositions to the aphanitic kimberlite might arise by a mixing process involving a protokimberlite, generated as a partial melt from a carbonated lherzolite source at a pressure greater than 7.0 GPa. After fractionation of olivine from this melt during ascent, the melt mixes at shallower depths with carbonate-rich magmas that cause desilication. These authors claim that evidence for such mixing is recorded in the macrocrysts in the kimberlite. In the case of the Wesselton aphanitic kimberlite, however, megacrysts are absent, and there is no indication of any participation of a carbonate-rich magma in the low CO_2 contents of this rock (Edgar et al., 1988, their Table 1). The relationship between the Type I macrocrystic Wesselton kimberlite and the aphanitic variety is not clear (Edgar et al., 1988), but there is no evidence from the olivine macrocrysts or from the chemical composition of this rock that a carbonate-rich magma was involved in its genesis.

The results of the present study offer an alternative explanation for these SiO_2-poor, CaO-rich kimberlites, namely, that they represent protokimberlite derived from partial melting of a nonlherzolite source, possibly over a range of depths greater than those of more SiO_2-rich CaO-poor kimberlites formed as partial melts of a lherzolite source.

If diamonds are xenocrystal phases in kimberlite, and with the assumption that kimberlites do not all originate at the same depth (see Mitchell, 1986), the hypothesis that diamond-bearing kimberlites of compositions similar to the Wesselton aphanitic kimberlite are derived from deeper levels can be useful in diamond exploration. Such kimberlite magmas will ascend and may pass through a much larger volume of potentially diamond-bearing mantle than more SiO_2-rich kimberlites from shallower sources. Unfortunately, if any relationship exists between the abundance of diamonds and the chemical composition of their host kimberlite, it has not been revealed to the scientific body public.

Ascent of the aphanitic kimberlite magma

Ascent of the aphanitic kimberlite magma may be modeled from the present study and from the one performed at lower pressure (Edgar et al., 1988). The principal differences between the lowest pressure experiments of this study (5.0 GPa), and those of the highest pressure of the latter study (4.0 GPa) is the presence of olivine + spinel at the liquidus at about 1450 °C at 4.0 GPa and of olivine + garnet but no spinel within 25 °C of the liquidus at about 1500 °C and 6.0 GPa (Fig. 4). Extrapolation of the liquidus of the present study to 4.0 GPa indicates a temperature about 50 °C greater than that determined in the previous study. This discrepancy may be the result of several factors, including the use of different apparatus for both studies, variation in the precision and accuracy of the temperature (or pressure) calibration, or transformations involving distribution of Al between Al-poor garnet + Al-rich quench clinopyroxene at high pressure and spinel + Al-poor clinopyroxene at lower pressure.

The data given here suggest that the aphanitic kimberlite ascended from its source region, possibly as deep as 330+ km (13.0 GPa) or as shallow as about 300 km (10.0 GPa) in the mantle. On ascent the magma may have formed at conditions represented by the liquidus (Fig. 4), where olivine ± garnet may have crystallized. (The possibility of clinopyroxene as an additional assemblage based on the quench phase in the experiments cannot be ignored.) At about 1500 °C and a depth of approximately 150 km (equivalent to below 5.0–6.0 GPa but above 4.0 GPa), garnet and Al-rich clinopyroxene (represented as a quench phase in the experiments) transformed to spinel and Al-poor clinopyroxene. On the basis of the lower pressure experiments (Fig. 1a of Edgar et al., 1988) the temperature at this depth may have been $1300 < T < 1400$ °C. On further cooling to about 50 km (>1.0 GPa), the magma cooled to below 1300 °C, on the basis of the absence of clinopyroxene and the presence of monticellite in the aphanitic kimberlite. Rapid uprise and cooling pro-

duced a matrix of olivine (now as serpentine), monticellite, spinel, calcite, and other phases such as phlogopite, formed at P-T conditions lower than those used by Edgar et al. (1988).

Acknowledgments

We are grateful to E.M.W. Skinner for donating the aphanitic kimberlite from Wesselton. The technical help of R. Tronnes at the University of Alberta multianvil laboratory and the assistance of R.L. Barnett, J. Forth, D.M. Kingston, and L. O'Connor at the University of Western Ontario is gratefully acknowledged. Versions of this manuscript were read by G. Brey, R.H. Sutcliffe, and D. Vukadinovic. Discussions with N.M.S. Rock, W.R. Taylor, and R. Ramsey, at the University of Western Australia, and especially C.J. Hatton of the Anglo-American Research Corporation proved very helpful. R. Wendlandt and two anonymous reviewers made many helpful comments. This research was financially supported by De Beers Consolidated Mines and by operating and major installation grants to the senior author.

References cited

Boettcher, A.L., Robertson, J.K., and Wyllie, P.J. (1980) Studies in synthetic carbonate systems: Solidus relationships for CaO-MgO-CO_2-H_2O to 40 kbar and CaO-MgO-SiO_2-CO_2-H_2O to 10 kbar. Journal of Geophysical Research, 85, 6937–6943.

Bohlen, S.R., and Boettcher, A.L. (1982) The quartz-coesite transition: A precise determination and the effect of other components. Journal of Geophysical Research, 87, 7073–7078.

Brey, G., Brice, W.P., Ellis, D.J., Green, D.H., Harris, K.L., and Ryabchikov, I.D. (1984) Pyroxene-carbonate reactions in the upper mantle. Earth and Planetary Sciences Letters, 62, 63–74.

Bulanova, G.P. (1986) Compositional evolution of syngenetic inclusions of ultrabasic association in Yukatian diamond. Extended Abstracts, 4th International Kimberlite Conference, p. 371–373. Geological Society of Australia, Perth.

Canil, D., and Scarfe, C.M. (1990) Phase relations in peridotite + CO_2 systems to 12 GPa: Implications for the origin of kimberlite and carbonate stability in the Earth's upper mantle. Journal of Geophysical Research, 95, 15805–15816.

Clement, C.R., Skinner, E.M.W., and Scott-Smith, B.H. (1984) Kimberlite redefined. Journal of Geology, 92, 223–228.

Dawson, J.B., and Stephens, W.E. (1975) Statistical analysis of garnets from kimberlites and associated xenoliths. Journal of Geology, 83, 589–607.

Edgar, A.D., Arima, M., Baldwin, D.K., Bell, D.R., Shee, S.R., Skinner, E.M.W., and Walker, E.C. (1988) High-pressure–high-temperature melting experiments on a SiO_2-poor aphanitic kimberlite from the Wesselton mine, Kimberley, South Africa. American Mineralogist, 73, 524–533.

Eggler, D.H. (1975) Peridotite-carbonate relations in the system CaO-MgO-SiO_2-CO_2. Carnegie Institution of Washington Year Book 74, 468–474.

——— (1978) The effect of CO_2 upon partial melting of peridotite in the system Na_2O-CaO-Al_2O_3-MgO-SiO_2-CO_2-H_2O to 35 kilobars, with an analysis of melting in a peridotite-H_2O-CO_2 system. American Journal of Science, 278, 305–343.

Eggler, D.H., and Baker, D.R. (1982) Reduced volatiles in the system C-O-H. Implications to mantle melting fluid formation and diamond genesis. In S. Akimoto and M. Manghnani, Eds., High pressure research in geophysics, p. 237–250. Tokyo Center for Academic Publications, Tokyo.

Eggler, D.H., and Wendlandt, R.F. (1979) Experimental studies on the relationship between kimberlite magma and partial melting of peridotite. In F.R. Boyd and H.O.A. Meyer, Eds., Kimberlites, diatremes and diamonds: Their geology, petrology and geochemistry, p. 331–378. American Geophysical Union, Washington, DC.

Ford, C.E. (1978) Platinum-iron alloy sample containers for melting experiments on iron-bearing rocks, minerals and related systems. Mineralogical Magazine, 42, 271–275.

Hall, H.T. (1971) Fixed points near room temperature. In E.C. Lloyd, Ed., Accurate characterization of the high pressure environment, N.B.S. Special Publication 326, p. 313–314. U.S. Government Printing Office, Washington, DC.

Hatton, C.J., and Gurney, J.J. (1987) Roberts Victor eclogites and their relation to the mantle. In P.H. Nixon, Ed., Mantle xenoliths, p. 453–464. Wiley, Chichester, U.K.

Herzberg, C., Gasparik, T., and Sawamoto, H. (1990) Origin of mantle peridotite: Constraints from melting experiments to 16.5 GPa. Journal of Geophysical Research, 95, 15779–15803.

Holman, C.G. (1975) Phase diagrams of Bi up to 140 kb. Journal of the Physics and Chemistry of Solids, 36, 1254–1269.

Huang, W.I., and Wyllie, P.J. (1984) Carbonation reactions for mantle lherzolite and harzburgite. 27th International Geological Congress, Proceedings 9, 455–473.

Irifune, T., Hibberson, W.O., and Ringwood, A.E. (1989) Eclogite-garnetite transformation at high pressures and its bearing on the occurrence of garnet inclusions in diamond. In J. Ross et al., Eds., Kimberlites and related rocks, vol. 2, p. 877–882. Geological Society of Australia, Carlton, Australia.

Kushiro, I. (1969) The system forsterite-diopside-silica with and without water at high pressures. American Journal of Science, 267A, 269–294.

Lloyd, F.E. (1987) Characterization of mantle metasomatic fluids in spinal lherzolites and alkali clinopyroxeneites from the West Eifel and South West Uganda. In M.A. Menzies and C.J. Hawkesworth, Eds., Mantle metasomatism, p. 91–124. Academic, London.

Luth, R.W., Virgo, D., Boyd, F.R., and Wood, B.J. (1990) Ferric iron in mantle-derived garnets: Implications for thermobarometry and for the oxidation state of the mantle. Contributions to Mineralogy and Petrology, 104, 56–72.

McGetchin, T.R., and Besancon, J.P. (1973) Carbonate inclusions in mantle-derived pyropes. Earth and Planetary Science Letters, 18, 408–410.

Mitchell, R.H. (1986) Kimberlites, 442 p. Plenum, New York.

O'Neill, H.S.C., and Wall, V.J. (1987) The olivine-orthopyroxene-spinel oxygen geobarometer, the nickel precipitation curve, and the oxygen fugacity of the Earth's upper mantle. Journal of Petrology, 28, 1169–1191.

Olafsson, M., and Eggler, D.H. (1983) Phase relations of amphibole, amphibole-carbonate and phlogopite-carbonate peridotite: Petrologic constraints on the asthenosphere. Earth and Planetary Science Letters, 64, 303–315.

Ringwood, A.E. (1989) Composition and evolution of the mantle. In J. Ross et al., Eds., Kimberlites and related rocks, vol. 1, p. 457–485. Geological Society of Australia, Carlton, Australia.

Shee, S.R. (1986) The petrogenesis of the Wesselton mica kimberlites, Kimberley, South Africa, 220 p. Ph.D. thesis, University of Capetown, Capetown, South Africa.

Susaki, J., Akaogi, M., Akimoto, S., and Shimomira, O. (1985) Garnet-perovskite transition in $CaGeO_3$: *In situ* X-ray measurements using synchrotron radiation. Geophysics Research Letters, 12, 729–732.

Takahashi, E. (1986) Melting of dry peridotite KLB-1 up to 16 GPa: Implications on the origin of peridotitic upper mantle. Journal of Geophysical Research, 91, 9367–9382.

Wendlandt, R.F., and Eggler, D.H. (1980a) The origin of potassic magmas. II. The stability of phlogopite in natural spinel lherzolite and in the system $KAlSiO_4$-MgO-SiO_2-H_2O-CO_2 at high pressures and high temperatures. American Journal of Science, 280, 421–458.

——— (1980b) The origin of potassic magmas. I. Melting relations in the system $KAlSiO_4$-Mg_2SiO_4-SiO_2 and $KAlSiO_4$-MgO-SiO_2-CO_2 to 30 kilobars. American Journal of Science, 280, 385–420.

Wyllie, P.J. (1977) Mantle fluid compositions buffered in peridotite-CO_2-H_2O. Journal of Geology, 85, 187–208.

——— (1978) Mantle fluid compositions buffered in peridotite-CO_2-H_2O by carbonates, amphiboles and phlogopite. Journal of Geology, 86, 687–713.

——— (1979a) Magmas and volatile components. American Mineralogist, 64, 469–500.

——— (1979b) Kimberlite magmas from the system peridotite-CO_2-H_2O. 2nd International Kimberlite Conference, p. 319–329. AGU, Washington, DC.

——— (1980) The origin of kimberlite. Journal of Geophysical Research, 85, 6902–6910.

Wyllie, P.J., and Huang, W.L. (1976) Carbonation and melting reactions in the system CaO-MgO-SiO_2-CO_2 at mantle pressures with geophysical and petrological applications. Contributions to Mineralogy and Petrology, 54, 79–100.

Yagi, T., and Akimoto, S.L. (1976) Direct determination of the coesite-stishovite transition by in situ X-ray measurements. Tectonophysics, 35, 259–270.

Yagi, T., Akaogi, M., Shimomura, O., Susuki, T., and Akimoto, S. (1987) In situ observation of the olivine-spinel phase transformation in Be_2SiO_4 using synchrotron radiation. Journal of Geophysical Research, 92, 6207–6213.

Manuscript received November 7, 1991
Manuscript accepted September 16, 1992